



A Bioinspired and Hierarchically Structured Shape-Memory Material

Citation

Cera, Luca, Grant M Gonzalez, Qihan Liu, Suji Choi, Christophe O Chantre, Juncheol Lee, Rudy Gabardi, Myung Chul Choi, Kwanwoo Shin, and Kevin Kit Parker. 2021. "A Bioinspired and Hierarchically Structured Shape-Memory Material." *Nature Materials* 20 (2): 242–49. <https://doi.org/10.1038/s41563-020-0789-2>.

Published version

<https://doi.org/10.1038/s41563-020-0789-2>

Link

<https://nrs.harvard.edu/URN-3:HUL.INSTREPOS:37370961>

Terms of use

This article was downloaded from Harvard University's DASH repository, and is made available under the terms and conditions applicable to Other Posted Material (LAA), as set forth at

<https://harvardwiki.atlassian.net/wiki/external/NGY5NDE4ZjgzNTc5NDQzMGIzZWZhMGFIOWI2M2EwYTg>

Accessibility

<https://accessibility.huit.harvard.edu/digital-accessibility-policy>

Share Your Story

The Harvard community has made this article openly available. Please share how this access benefits you. [Submit a story](#)

Supporting Information

A Bioinspired and Hierarchically Structured Shape Memory Material

By Luca Cera, Grant M. Gonzalez, Qihan Liu, Suji Choi, Christophe O. Chantre, Juncheol Lee, Myung C. Choi, Rudy Gabardi, Kwanwoo Shin, and Kevin Kit Parker*

Table of contents

11	Supplementary Video 1. Shape memory fibers	S2
12	Supplementary Video 2. Shape memory 3D printed scaffold	S2
13	Supplementary Figure 1. Determination of keratin concentration by using the	
14	Bradford assay	S2
15	Supplementary Figure 2. Raman spectroscopy of a dry sample of the	
16	extracted keratin	S3
17	Supplementary Figure 3. α-helix coiled-coil structure characterization using	
18	circular dichroism	S3
19	Supplementary Figure 4. SDS-Page of the extracted keratin solution	S4
20	Supplementary Figure 5. Pulling fibers from keratin solution	S5
21	Supplementary Figure 6. Keratin fibers wet-spinning protocol and set-up	S5
22	Supplementary Figure 7. Tuning of keratin fiber diameter	S6
23	Supplementary Figure 8. 2D WAXS pattern comparison between the unstretched	
24	keratin fiber and wool	S7
25	Supplementary Figure 9. WAXS Equatorial scattering profiles of unstrained	
26	and strained keratin fibers	S8
27	Supplementary Figure S10. Ashby plots comparing the mechanical properties of	
28	literature reported WTSM with the engineered SM keratin materials	S8
29	Supplementary Figure 11. Mechanical properties of isotropic casted keratin films	S9
30	Supplementary Table 1. Mechanical properties of literature reported WTSM	
31	materials Description of supplementary video material	S10
32	References	S11

34 **Supplementary Video 1. Shape memory fibers.**

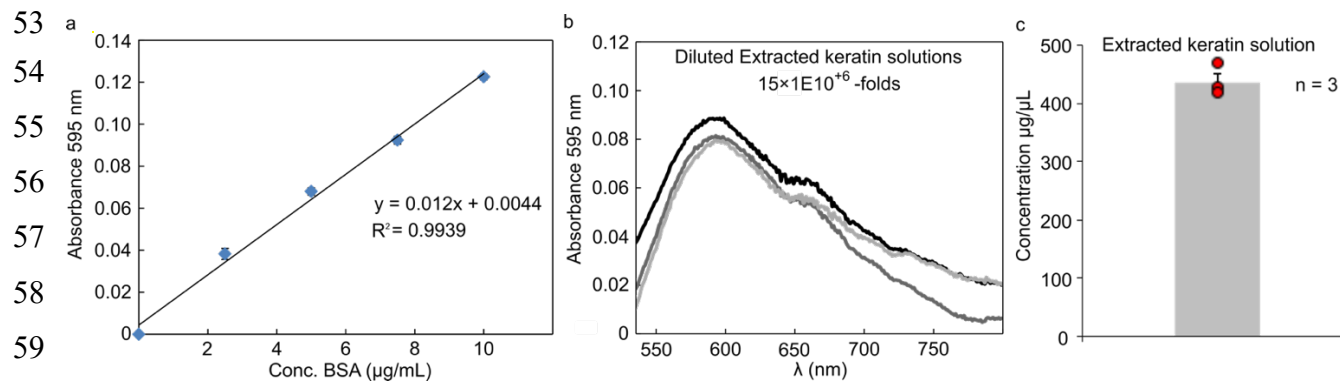
35 *Images shown in Figures 3g are taken from this video.*

36 The yarn was produced by manually twisting a fiber strand of same diameter size (~ 30
37 microns), which are blocked together with knots at both edges. The yarn is immersed into
38 deionized water for a few seconds, manually stretched while still in a wet state and kept under
39 load at room temperature for about 10 minutes. When weights are removed to allow the yarn to
40 relax, no visible change in length between the stretched and relaxed form is observed by the
41 naked eye. To show the ability of the yarn to recover its original length nebulized water is
42 applied. Indeed, shrinking of the fibers leads to reshaping of the yarn to its original length only in
43 a few seconds.

45 **Supplementary Video 2. Shape memory 3D printed scaffolds.**

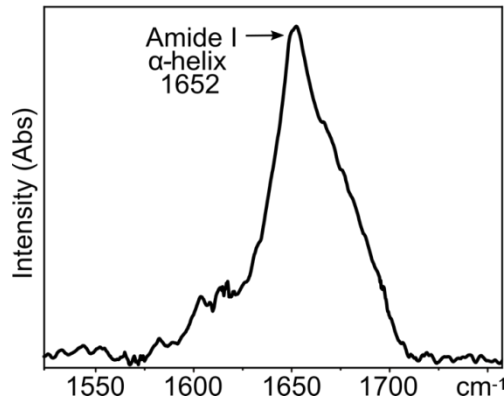
46 *Images shown in Figures 4f are taken from this video.*

47 The 3D printed star-shaped origami is locked in a rolled-tube temporary configuration and
48 hydrated to regain its original permanent architecture. This happens after a few seconds of
49 hydration, when the keratin rolled tube starts an unfolding process caused by fluttering of the
50 bended surfaces. Closure of the final origami is achieved as the star edges are reformed and fold
51 back in a cooperative fashion.

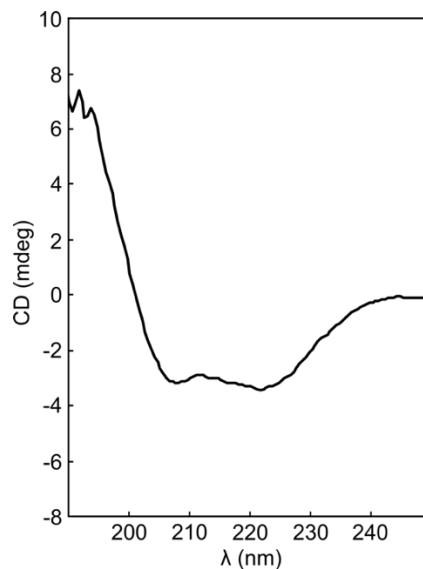


61 **Supplementary Figure 1. Determination of keratin concentration by using the Bradford**
62 **assay.** a) Standard curve obtained from known bovine serum albumin (BSA) concentrations
63 using the Bradford assay (n = 3 sample tested per each concentration of BSA). b) UV-Vis
64 absorption spectra of $15 \times 10^{10} + 6$ diluted samples of extracted keratin (n = 3 independent keratin

65 extraction batches tested). c) Bar graph with associated scattering plot showing the protein
66 concentration of the extracted keratin solution of 401.7 ± 15 mg/mL ($n = 3$ independent keratin
67 extraction batches tested). Data are presented as mean values \pm SEM.



77 **Supplementary Figure 2. Raman spectroscopy of a dry sample of the extracted keratin.** The
78 analysis was performed on a keratin sample purified via dialysis against water (1 L \times 3) over 48
79 hours and freeze-dried. The retainment of the α -helix secondary structure during extraction is
80 supported by the presence of the characteristic band at 1652 cm^{-1} .¹



92 **Supplementary Figure 3. α -helix coiled-coil structure characterization using circular**
93 **dichroism CD.** Spectrum of the extracted keratin solution in water at pH 5.6 (0.2 mg/mL) and
94 using a cuvette with a 5 mm path-length. The presence of the positive band at 192 nm and the
95 negative bands at 208 and 222 nm supports the α -helix conformation of keratin in solution.²

96 Furthermore, the intensity ratio between the band at 222 nm and the band at 208 nm ($R_2 =$
97 $222\text{nm}/208\text{nm}$) is greater than 1, indicating the arrangement of the paired α -helices in the coiled-
98 coil architecture.³

99

100

101

102

103

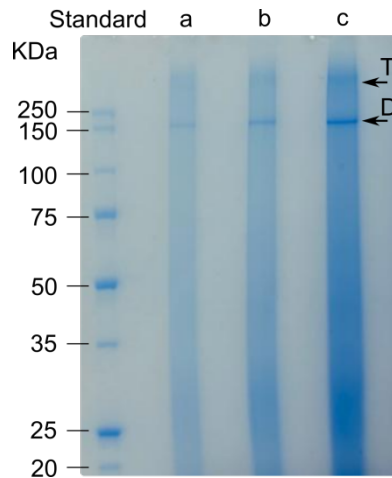
104

105

106

107

108



109 **Supplementary Figure 4. SDS-Page of the extracted keratin solution.** Concentration-

110 dependent SDS-Page analysis carried out on the extracted keratin solution, using a 10%

111 acrylamide gel and a Tris/Glycine/SDS running buffer. Samples were prepared by mixing 5 μL

112 of a 50-folds diluted solution of the extracted keratin (diluted in a 3M LiBr water solution) with

113 a) 80 μL , b) 40 μL and c) 20 μL of Laemmli buffer containing DTT (50 mM). After gel fixation

114 using a water solution of isopropyl alcohol (25% v/v) and acetic acid (10% v/v), the gel was

115 stained using a water solution of acetic acid (10 % v/v) and Coomassie blue 60 (mg/L). The

116 presence of the main band at ~150 kDa belonging to α -helix dimer (D) and the one at higher

117 molecular weights, belonging to the tetramer (T), supports the successful preservation of the

118 coiled-coil structure during extraction and few degradation products.⁴ Although no characteristic

119 bands in the 40-60 kDa range are observed, Angora wool keratin is known to be a heterodimeric

120 polymer.⁵ The SDS-Page experiment was carried out 3 times for a Laemmli solution

121 concentration of 40 μL .

122

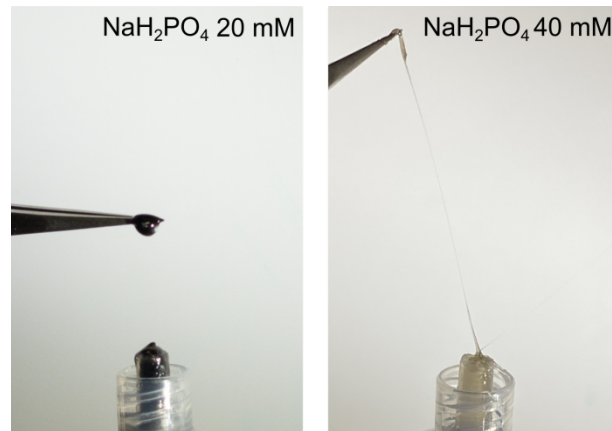
123

124

125

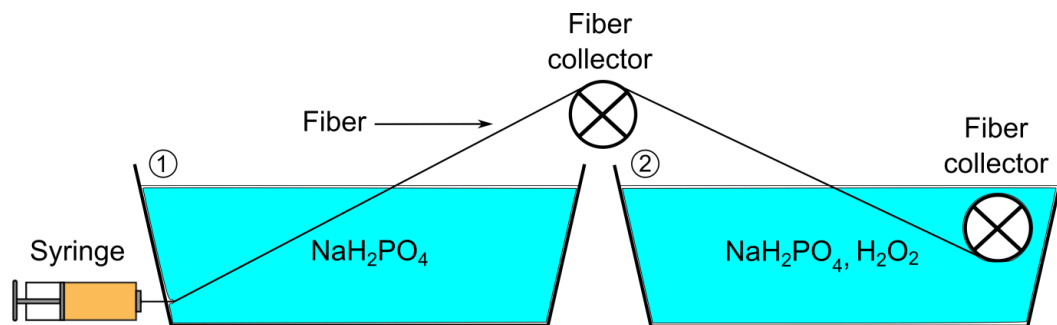
126

127
128
129
130
131
132
133
134



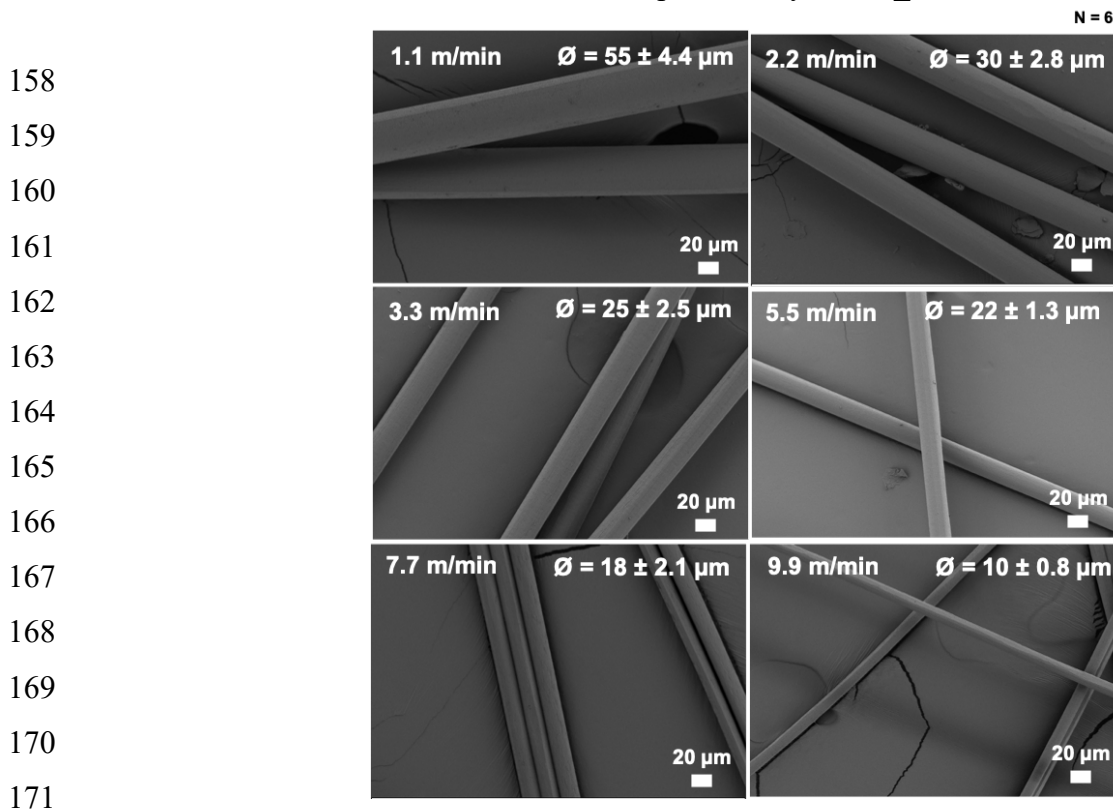
135 **Supplementary Figure 5. Pulling fibers from keratin solution.** Photographs of the extracted
136 keratin solutions (401.7 mg/mL) containing 20 mM (left) and 40 mM (right) of NaH_2PO_4 . At
137 concentration of NaH_2PO_4 lower than 40 mM, the lower degree of keratin self-assembly hinders
138 fiber formation when the solution is pulled with a tweezer.

139
140
141
142
143
144
145



146 **Supplementary Figure 6. Keratin fibers wet-spinning protocol and set-up.** Schematic of the
147 wet-spinning platform used to produce keratin fibers. The platform consists of a syringe pump
148 and two coagulation baths placed in series with independent polytetrafluoroethylene (PTFE)
149 collectors. At room temperature, the keratin dope is infused at a $10 \mu\text{L}/\text{min}$ of rate into the first
150 coagulation bath containing a water solution of NaH_2PO_4 , at a pH lower than the average keratin
151 isoelectric point (0.4 M, pH 4.3).⁶ A needle of 27 gauge is used (needle length 3 cm, McMaster-
152 Car). Fibers are collected after the first coagulation bath and continuously drawn into the second
153 coagulation bath containing a water solution of NaH_2PO_4 (0.8 M) and H_2O_2 (1%). The two
154 reaction steps were located in different and sequential baths to allow for the complete
155 coagulation of the protein before forming the disulfide covalent network, because the H_2O_2 -
156 assisted oxidation occurs with a fast kinetic.⁷

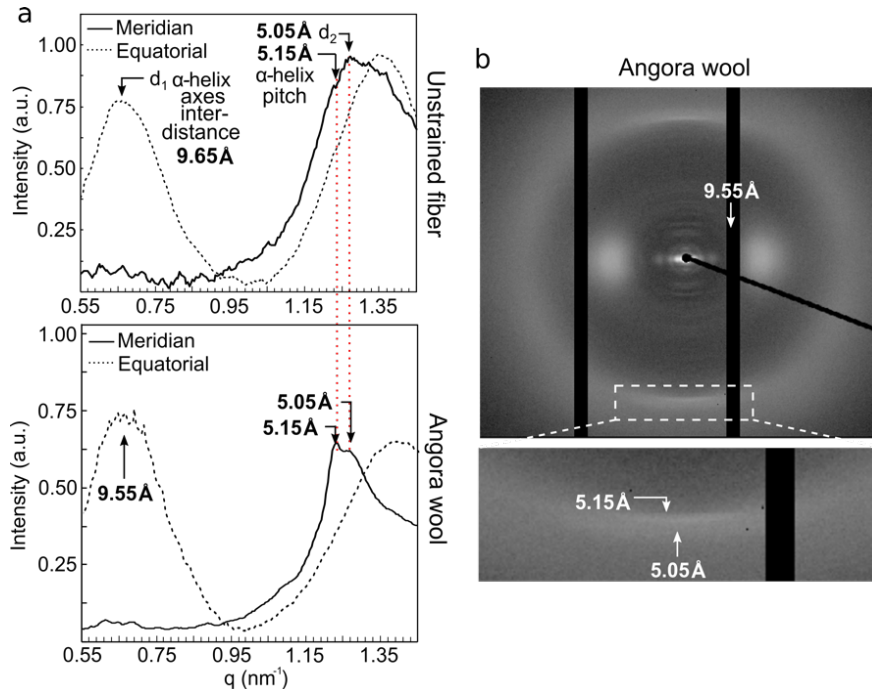
157



172 **Supplementary Figure 7. Tuning of keratin fiber diameter.** SEM micrographs of keratin
173 fibers obtained at different collection speeds. As shown in the image, the fiber diameter can be
174 finely tuned by increasing the speed of the second collector. Furthermore, the small standard
175 error of the mean calculated for the average diameter size shows high accuracy and stability of
176 the spinning process (n = 6 fibers tested per experimental condition; data are presented as mean
177 values with experimental errors +/- calculated as SEM).

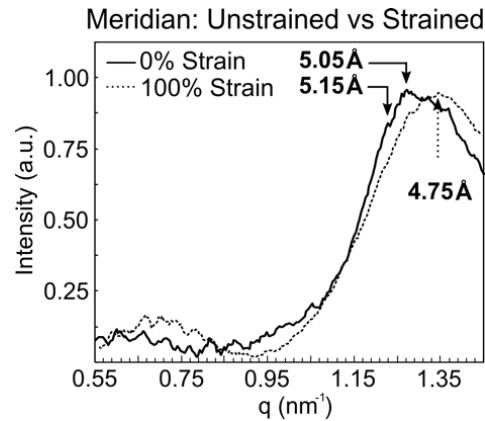
178
179
180
181
182
183
184
185
186
187
188
189
190

191
192
193
194
195
196
197
198
199
200
201
202
203
204
205
206
207
208
209
210
211
212
213
214
215
216
217
218
219
220
221
222
223



Supplementary Figure 8. 2D WAXS pattern comparison between the unstretched keratin fiber and wool. a) Comparison of the meridian and equatorial scattering profiles between the regenerated keratin fiber and Angora wool. The meridian shoulder at 5.15 Å and maximum at 5.05 Å of the regenerated fiber match with the meridian and off-meridian reflections of Angora wool (respectively), suggesting the presence of coiled-coils aligned along the fiber axis. Compared to the natural fiber however, the meridian reflections of the regenerated keratin fiber are broader, indicating the coiled-coils to be less crystalline and have a lower degree of alignment. b) 2D WAXS pattern of Angora wool showing the characteristic reflections at 9.55 Å belonging to the α -helix axes inter-distance, and the meridian and off-meridian reflections at 5.15 Å and 5.05 Å belonging to the α -helix pitch projection.^{8,9}

224
225
226
227
228
229
230
231



232 **Supplementary Figure 9. WAXS Equatorial scattering profiles of unstrained and strained**
233 **keratin fibers.** Meridian scattering profiles of the unstrained and strained keratin fibers. The
234 decrease in intensity of the 5.15 Å and 5.05 Å peaks supports the uncoiling of the alpha-helices
235 upon fiber stretching.

236

237

238

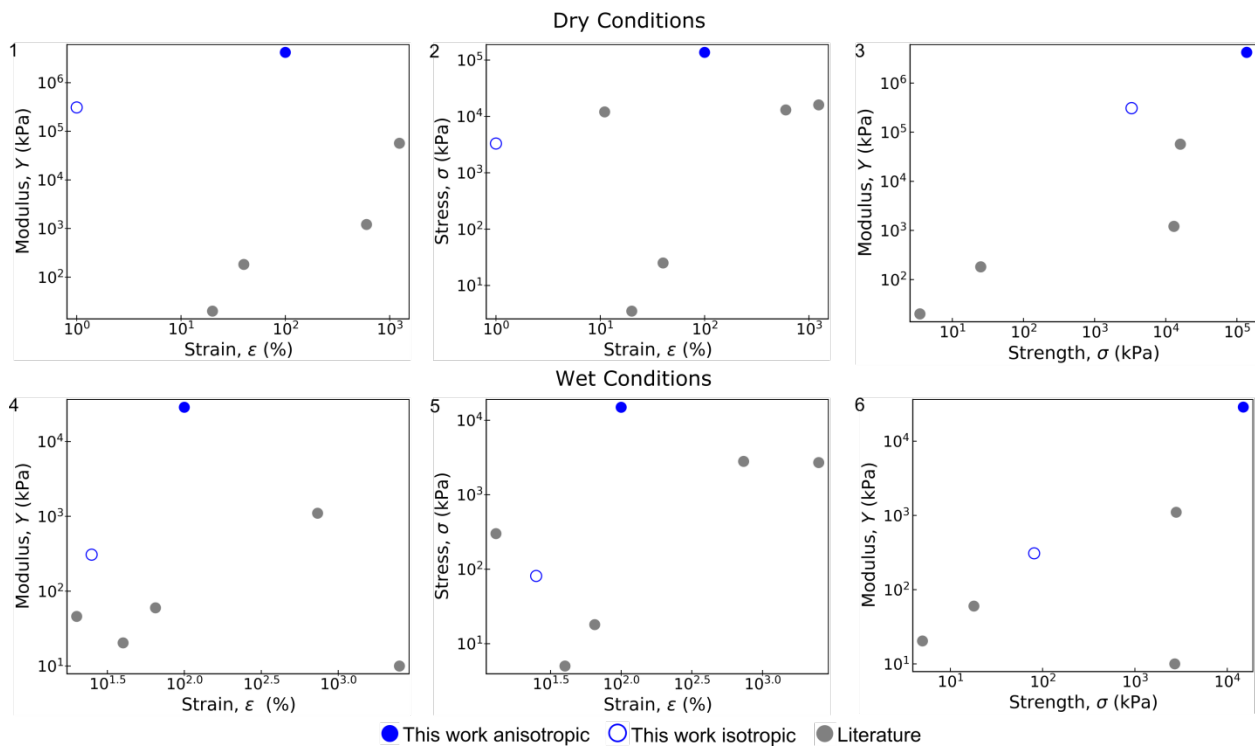
239

240

241

242

243



244

245

246

247

248

249

250

251

252

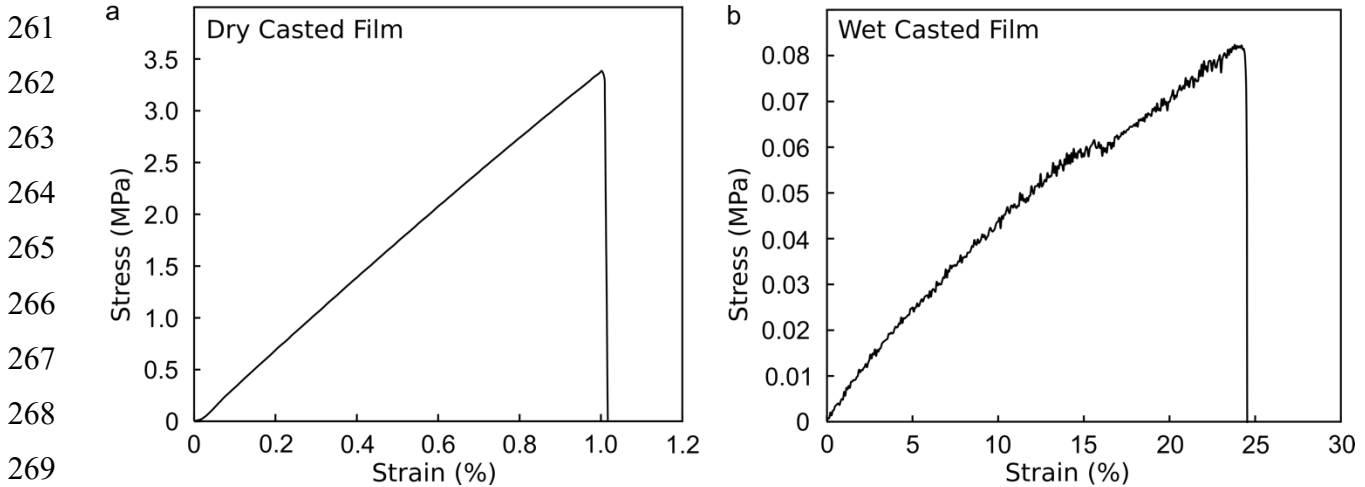
253

254

Supplementary Figure S10. Ashby plots comparing the mechanical properties of literature
reported WTSM with the engineered SM keratin materials. Ashby plots correlating Young's
modulus, tensile stress and max strain of the literature reported WTSM materials and the
engineered keratin SM material both in dry and wet conditions. The graphs support the

255 importance of the anisotropic organization of the protofibrils in realizing the shape memory
256 effect and allowing for the high mechanical performances of the material. Compared to the
257 extruded material, the thin films are much more brittle and have lower tensile strength, both in
258 dry and wet conditions. These films have mechanical properties more similar to literature
259 reported WTSM materials.

260



270 **Supplementary Figure 11. Mechanical properties of isotropic casted keratin films.**

271 Representative stress-strain plots (representative of $n = 3$ curves) of cast keratin films ($25 \times 5 \times 0.3$
272 mm) in dry (left) and wet (right) conditions. Films were fabricated by casting the extracted
273 keratin solution into acrylic moulds and inducing protein coagulation and cross-linking using a
274 NaH_2PO_4 (0.8 M) and H_2O_2 (1% v/v) water bath. Compared to the extrusion process, the cast
275 keratin material is much more brittle and has a lower tensile strength, both in dry (tensile
276 strength of 3.29 ± 0.43 MPa and strain to failure of 1.02 ± 0.02 %) and wet (tensile strength of
277 81.5 ± 8.1 KPa and strain to failure of 25.3 ± 2.3 %) conditions. The decrease in mechanical
278 performances due to the isotropic nanostructure of the casted film underscores the importance of
279 protofibrils alignment to realize the shape memory effect. Data are presented as mean values,
280 with experimental errors \pm calculated as SEM.

281

282

283

284

285

Chemical System	Trigger	Tensile Stress. kPa		Young's Modulus kPa		Max Strain (dry-wet)	Publication	Year
		Dry	Wet	Dry	Wet			
This Work (Anisotropic)	Water	>137,180	14,940	4.2×10^6	28.7×10^3	100-100%	/	/
This work (Isotropic)	Water	3,300	81	309000	308	1-25%		
Poly(butylene 2,5-furandicarboxylate)/Vinyl ¹⁰	Water	25	5	182	20.36	40-40%	J. Mater. Chem. B	2019
tetra-poly(ethylene glycol)-based ¹¹	Water	13,000	2,700	1,210	10	600-2501%	Polym. Chem.	2019
*Silk-based ¹²	Water	3.5	/	20	46	20%	Adv. Healthcare Mater.	2017
Gelatin ¹³	Water	12000	300			11-13%	J. Mater. Chem. B	2017
Bovine Serum Albumin ¹⁴	Water	/	18	/	60	65%	Nat. Commun	2019
Thermoplastic Polyurethane ¹⁵	Water	>16,000	2,800	56,800	1,100	1240-735%	RSC Adv.	2013

286

287 **Supplementary Table 1. Mechanical properties of literature reported WTSM materials.**

288 Compared to the literature reported examples, both in dry and wet conditions, the tensile stress of
 289 our engineered material is one order of magnitude greater (dry = 137.18 ± 1.03 MPa, wet = 14.94
 290 ± 0.46 MPa). The Young's modulus reaches even two orders of magnitude of difference, when in
 291 dry conditions (dry = 4.18 ± 0.10 GPa, wet = 28.7 ± 2.45). * The data are for compressive
 292 mechanical tests.

293

294

295

296

297

298

299

300

301

302 **References**

- 1 Paquin, R. & Colomban, P. *J. Raman Spectrosc.* **38**, 504-514 (2007).
- 2 Rodger A. *Far UV Protein Circular Dichroism. In: Roberts G.C.K. (eds) Encyclopedia of Biophysics.* (Springer, Berlin, Heidelberg 2013).
- 3 Smith, A. M., Banwell, E. F., Edwards, W. R., Pandya, M. J. & Woolfson D. N. Engineering Increased Stability into Self-Assembled Protein Fibers. *Adv. Funct. Mater.* **16**, 1022-1030 (2006).
- 4 Bernot, K. M., Lee, C.-H. & Coulombe, P. A. A small surface hydrophobic stripe in the coiled-coil domain of type I keratins mediates tetramer stability. *J. Cell Biol.* **168**, 965-974 (2005).
- 5 Sahajpal, V., Goyal, S., Singh, K. & Thakur, V. Dealing wildlife offences in India: role of the hair as physical evidence. *Int. J. Trichology* **1**, 18-26 (2009).
- 6 Li, Q., Brady, P. R. & Wang, X. Influence of pH on Hygral Expansion, Relaxation Shrinkage and Extensibility of Wool Fabric. *Fiber Polym.* **8**, 230-233 (2007).
- 7 Scott, D. L., Bradley, W. S. & Anderson, D. Kinetics and mechanism of the reaction of cysteine and hydrogen peroxide in aqueous solution. *J. Pharm. Sci.* **94**, 304-316 (2005).
- 8 Soomro, A., Alsop, R. J., Negishi, A., Kreplak, L., Fudge, D., R. Kuczmarski, E., Goldman, R. D. & Rheinstädter, M. C. *J. R. Soc. Interface* **14**, 20170123 (2017).
- 9 Busson, B., Briki, F. & Doucet, J. Side-Chains Configurations in Coiled Coils Revealed by the 5.15-Å Meridional Reflection on Hard α -Keratin X-Ray Diffraction Patterns. *J. Struct. Biol.* **125**, 1-10 (1999).
- 10 Guo, Y., Lv, Z., Huo, Y., Sun, L., Chen, S., Liu, Z., He, C., Xiaoping, Bi., Fanc, X. & You, Z. A biodegradable functional water-responsive shape memory polymer for biomedical applications. *J. Mater. Chem. B*, **7**, 123-132 (2019).
- 11 Tian, T., Wang, J., Wu, S., Shao, Z., Xiang, T. & Zhou, T. A body temperature and water-induced shape memory hydrogel with excellent mechanical properties. *Polym. Chem.* **10**, 3488-3496 (2019).
- 12 Brown, J. E., Moreau, J. E., Berman, A. M., McSherry, H. J., Coburn, J. M., Schmidt, D. F. & Kaplan, D. L. Shape Memory Silk Protein Sponges for Minimally Invasive Tissue Regeneration. *Adv. Healthcare Mater.* **6**, 1600762, (2017).

-
- 13 R. Zamani Alavijeh, R. Z., Shokrollahi, P. & Barzin J. A thermally and water activated shape memory gelatin physical hydrogel, with a gel point above the physiological temperature, for biomedical applications *J. Mater. Chem. B* **5**, 2302-2314 (2017).
 - 14 Luai R. Khoury, L. R. & Popa, I. Chemical unfolding of protein domains induces shape change in programmed protein hydrogels. *Nat. Commun.* **10**, 5439 (2019).
 - 15 Gu, x. & Mather P. T. Water-triggered shape memory of multiblock thermoplastic polyurethanes (TPUs). *RSC Adv.*, **3**, 15783-15791 (2013).